

# Spontaneous Resolution of a Racemic Nickel(II) Complex and Helicity Induction via Hydrogen Bonding: The Effect of Chiral Building Blocks on the Helicity of One-Dimensional Chains

Guang-Chuan Ou, Long Jiang, Xiao-Long Feng, and Tong-Bu Lu\*

MOE Key Laboratory of Bioinorganic and Synthetic Chemistry/State Key Laboratory of Optoelectronic Materials and Technologies/School of Chemistry and Chemical Engineering, Sun Yat-Sen University, Guangzhou 510275, China

Received October 31, 2007

The reactions of a racemic four-coordinated nickel(II) complex  $[\text{Ni}(\alpha\text{-rac-L})](\text{ClO}_4)_2$  (containing equal amount of *SS* and *RR* enantiomers) with *l*- and *d*-phenylalanine in acetonitrile/water gave two less-soluble six-coordinated enantiomers of  $\{[\text{Ni}(f\text{-SS-L})(l\text{-Phe})](\text{ClO}_4)_n\}$  ( $\Delta\text{-1}$ ) and  $\{[\text{Ni}(f\text{-RR-L})(d\text{-Phe})](\text{ClO}_4)_n\}$  ( $\Lambda\text{-1}$ ), respectively. Evaporation the remaining solutions gave two six-coordinated diastereomers of  $\{[\text{Ni}_3(f\text{-RR-L})_3(l\text{-Phe})_2(\text{H}_2\text{O})](\text{ClO}_4)_4\}_n$  (*a-2*) and  $\{[\text{Ni}_3(f\text{-SS-L})_3(d\text{-Phe})_2(\text{H}_2\text{O})](\text{ClO}_4)_4\}_n$  (*b-2*), respectively (L = 5,5,7,12,12,14-hexamethyl-1,4,8,11-tetraazacyclotetradecane,  $\text{Phe}^-$  = phenylalanine anion). The reaction of  $[\text{Ni}(\alpha\text{-rac-L})](\text{ClO}_4)_2$  with *d*- $\text{Phe}^-$  gave a conglomerate of *c-1*; in which, the *SS* and *RR* enantiomers preferentially coordinate to *l*- and *d*- $\text{Phe}^-$  respectively to give a racemic mixture of  $\Delta\text{-1}$  and  $\Lambda\text{-1}$ , and the spontaneous resolution occurs during the reaction, in which each crystal crystallizes to become enantiopure. Removing  $\text{Phe}^-$  from  $\Delta\text{-1}$  and  $\Lambda\text{-1}$  using perchloric acid gave two enantiomers of  $[\text{Ni}(\alpha\text{-SS-L})](\text{ClO}_4)_2$  (*S-3*) and  $[\text{Ni}(\alpha\text{-RR-L})](\text{ClO}_4)_2$  (*R-3*). Dissolving *S-3* and *R-3* in acetonitrile gave two six-coordinated enantiomers of  $[\text{Ni}(f\text{-SS-L})(\text{CH}_3\text{CN})_2](\text{ClO}_4)_2$  (*S-4*) and  $[\text{Ni}(f\text{-RR-L})(\text{CH}_3\text{CN})_2](\text{ClO}_4)_2$  (*R-4*), while dissolving  $[\text{Ni}(\alpha\text{-rac-L})](\text{ClO}_4)_2$  in acetonitrile gave a racemic twining complex  $[\text{Ni}(f\text{-rac-L})(\text{CH}_3\text{CN})_2](\text{ClO}_4)_2$  (*rac-4*).  $\Delta\text{-1}$  and  $\Lambda\text{-1}$  belong to supramolecular stereoisomers, which are constructed via hydrogen bond linking of  $[\text{Ni}(f\text{-SS-L})(l\text{-Phe})]^+$  and  $[\text{Ni}(f\text{-RR-L})(d\text{-Phe})]^+$  monomers to form 1D homochiral right-handed and left-handed helical chains, respectively. The reaction of *S-3* with *d*- $\text{Phe}^-$  gave  $\{[\text{Ni}(f\text{-SS-L})(d\text{-Phe})](\text{ClO}_4)_n\}$  (*5*), which shows a motif of a 1D hydrogen bonded zigzag chain instead of a 1D helical chain. Compound *a-2/b-2* contains dimers of  $\{[\text{Ni}(f\text{-RR-L})_2(l\text{-Phe})(\text{H}_2\text{O})]^{3+}/[\text{Ni}(f\text{-SS-L})_2(d\text{-Phe})(\text{H}_2\text{O})]^{3+}\}_n$  and 1D zigzag chains of  $\{[\text{Ni}(f\text{-RR-L})(l\text{-Phe})]^+\}_n/\{[\text{Ni}(f\text{-SS-L})(d\text{-Phe})]^+\}_n$ . The homochiral nature of  $\Delta\text{-1}/\Lambda\text{-1}$ , *a-2/b-2*, *S-3/R-3*, and *S-4/R-4* are confirmed by the results of circular dichroism (CD) spectra measurements.

## Introduction

The macrocyclic ligand, 5,5,7,12,12,14-hexamethyl-1,4,8,11-tetraazacyclotetradecane (L), was prepared 40 years ago by Curtis.<sup>1</sup> Its nickel(II) complexes exist as two diastereomers of *meso* and *rac* (racemic) forms.<sup>2</sup> In the *meso* form, the two asymmetric carbon atoms adopt opposite (*R* and *S*) configurations, while they adopt the same (*RR* or *SS*)

configuration in the *rac* form (Scheme 1). The two diastereomers can be separated by crystallization.<sup>1–3</sup> There are two isomers in four coordinated Ni(II) complexes: the yellow isomer of  $[\text{Ni}(\alpha\text{-rac-L})]^{2+}$  and the orange isomer of  $[\text{Ni}(\beta\text{-rac-L})]^{2+}$ . The two isomers can interconvert with each other in solution as the energy difference between the two isomers is very small,<sup>1</sup> so precise control the experimental conditions to form a defined isomer still remains difficult.

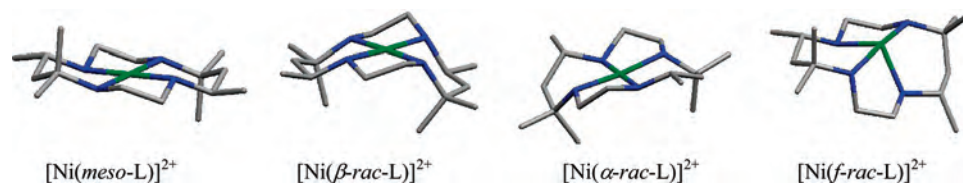
The separation of  $[\text{Ni}(\alpha\text{-rac-L})]^{2+}$  and  $[\text{Ni}(\beta\text{-rac-L})]^{2+}$  is necessary as they form different structures with organic ligands.<sup>4</sup> In our previous studies,<sup>4–6</sup> We found a simple

\* To whom correspondence should be addressed. Tel.: +86-20-84112921. E-mail address: lutongbu@mail.sysu.edu.cn.

(1) Curtis, N. F. *J. Chem. Soc. (A)* **1960**, 4409; **1965**, 924; **1967**, 2644.  
(2) (a) Curtis, N. F.; Curtis, Y. M.; Powell, E. J. K. *J. Chem. Soc. (A)* **1966**, 1015. (b) Warner, L. G.; Rose, N. J.; Busch, D. H. *J. Am. Chem. Soc.* **1967**, 89, 703. (c) Curtis, N. F.; Curtis, Y. M. *J. Chem. Soc. (A)* **1966**, 1653.

(3) Tait, A. M.; Busch, D. H. *Inorg. Synth.* **1976**, 18, 4.

(4) Jiang, L.; Feng, X. L.; Lu, T. B. *Cryst. Growth Des.* **2005**, 5, 1469.

Scheme 1. Coordination Geometries of *meso*-L and *rac*-L in Ni(II) Complexes<sup>a</sup>

<sup>a</sup> Only the *SS* form is shown.

method for the separation of  $[\text{Ni}(\alpha\text{-rac-L})](\text{ClO}_4)_2$  and  $[\text{Ni}(\beta\text{-rac-L})](\text{ClO}_4)_2$ ,<sup>4</sup> and we used  $[\text{Ni}(\alpha\text{-rac-L})]^{2+}$  and  $[\text{Ni}(\text{CN})_4]^{2-}$  as building blocks to construct a series of supramolecular isomers and stereoisomers of molecular square and 1D helical chains.<sup>5,6</sup> It is interesting to note that interchain solvents can affect the crystallizing forms of 1D helical chains  $\{[\text{Ni}(f\text{-rac-L})][\text{Ni}(\text{CN})_4]_n(\text{solvent})_n\}$ . In  $\{[\text{Ni}(f\text{-rac-L})][\text{Ni}(\text{CN})_4]_n(\text{H}_2\text{O})_{3n}\}$ , the interchain water molecules form hexameric water clusters of  $(\text{H}_2\text{O})_6$ , and the helical chains are separated by these water clusters, in which the interchain water clusters act like a “mirror plane” to allow the interchain chirality to propagate in an opposite manner to result in an achiral compound. In  $\{[\text{Ni}(f\text{-rac-L})][\text{Ni}(\text{CN})_4]_n(\text{MeCN})_n\}$ , the interchain hydrophobic interactions propagate the interchain chirality in a uniform way, leading to the formations of a chiral compound. It was also found that spontaneous resolution of  $[\text{Ni}(\alpha\text{-rac-L})]^{2+}$  occurred during the formations of 1D helical chains with  $[\text{Ni}(\text{CN})_4]^{2-}$ , and *RR*-L and *SS*-L exist in the right- and left-handed helical chains, respectively.<sup>6</sup>

Recently, many helical structures have been constructed using chiral<sup>7</sup> or achiral building blocks.<sup>8–11</sup> In many cases, right-handed and left-handed helices are obtained in equal

amounts as a racemate when racemic or achiral building blocks are used. In some cases, however, spontaneous resolution into enantiomeric chiral crystals occurs. Although spontaneous resolution was discovered 100 years ago,<sup>12</sup> it is still a relatively rare phenomenon,<sup>8</sup> and cannot be predicted because the laws of physics determining the processes are not yet fully understood.<sup>8b</sup> It has been found that interchain supramolecular interactions such as hydrogen bonds,  $\pi \cdot \cdot \cdot \pi$ , and hydrophobic interactions play important roles in the process of spontaneous resolution.<sup>6,8d,10d</sup>

As a continuance of our research on the constructions of chiral helical chains, and the factors that influence the construction and chirality of helical chains, as well as the phenomenon of spontaneous resolution of  $[\text{Ni}(\alpha\text{-rac-L})]^{2+}$ , a series of hydrogen bond linked chains with helical and zigzag motifs have been constructed. It was found that the monomers of  $[\text{Ni}(f\text{-SS-L})(l\text{-Phe})]^+$  and  $[\text{Ni}(f\text{-RR-L})(d\text{-Phe})]^+$  are connected through the intermolecular hydrogen bonds to generate 1D right-handed and left-handed homochiral helical chains, respectively (Phe<sup>−</sup> = phenylalanine anion). While similar intermolecular hydrogen bond linking of  $[\text{Ni}(f\text{-RR-L})(l\text{-Phe})]^+$  and  $[\text{Ni}(f\text{-SS-L})(d\text{-Phe})]^+$  monomers generate 1D zigzag chains instead of helical chain. Though many helical structures have been reported,<sup>5–11,13</sup> most of them are constructed through the coordination interactions of the organic ligand with suitable metal ions.<sup>5–11</sup> Helical polymers constructed via hydrogen bonding, which is a versatile and efficient strategy,<sup>13a</sup> are still rare, and only a few cases have been reported.<sup>13</sup> To our knowledge, 1D helical chains containing more than one kinds of chiral building blocks have not been reported so far. Herein, we report on the spontaneous resolution of a racemic nickel(II) complex  $[\text{Ni}(\alpha\text{-rac-L})]^{2+}$  with racemic *dl*-Phe<sup>−</sup>, and 1D hydrogen bonded homochiral *right*- and *left*-handed helical chains of  $\{[\text{Ni}(f\text{-SS-L})(l\text{-Phe})](\text{ClO}_4)_n\}$  and  $\{[\text{Ni}(f\text{-RR-L})(d\text{-Phe})](\text{ClO}_4)_n\}$ , as

(5) Jiang, L.; Lu, T. B.; Feng, X. L. *Inorg. Chem.* **2005**, *44*, 7056.

(6) Jiang, L.; Feng, X. L.; Su, C. Y.; Chen, X. M.; Lu, T. B. *Inorg. Chem.* **2007**, *46*, 2637.

(7) (a) Wen, H. R.; Wang, C. F.; Li, Y. Z.; Zuo, J. L.; Song, Y.; You, X. Z. *Inorg. Chem.* **2006**, *45*, 7032. (b) Wen, H. R.; Wang, C. F.; Zuo, J. L.; Song, Y.; Zeng, X. R.; You, X. Z. *Inorg. Chem.* **2006**, *45*, 582. (c) Wen, H. W.; Wang, C. F.; Song, Y.; Zuo, J. L.; You, X. Z. *Inorg. Chem.* **2005**, *44*, 9039. (d) Roth, A.; Koth, D.; Gottschaldt, M.; Plass, W. *Cryst. Growth Des.* **2006**, *6*, 2655. (e) Akitsu, T.; Einaga, Y. *Inorg. Chem.* **2006**, *45*, 9826. (f) Albrecht, M.; Dehn, S.; Raabe, G.; Fröhlich, R. *Chem. Commun.* **2005**, 5690. (g) Anokhina, E. V.; Jacobson, A. J. *J. Am. Chem. Soc.* **2004**, *126*, 3044. (h) Wu, C. D.; Ngo, H. L.; Lin, W. B. *Chem. Commun.* **2004**, 1588. (x) Cui, Y.; Ngo, H. L.; Lin, W. B. *Chem. Commun.* **2003**, 1388. (i) Johnson, J. A.; Kampf, J. W.; Pecoraro, V. L. *Angew. Chem., Int. Ed.* **2003**, *42*, 546. (j) Ellis, W. W.; Schmitz, M.; Arif, A. A.; Stang, P. J. *Inorg. Chem.* **2000**, *39*, 2547.

(8) (a) Siemeling, U.; Schepplmann, I.; Neumann, B.; Stammeler, A.; Stammeler, H.-G.; Frelek, J. *Chem. Commun.* **2003**, 2236. (b) Gao, E. Q.; Yue, Y. F.; Bai, S. Q.; He, Z.; Yan, C. H. *J. Am. Chem. Soc.* **2004**, *126*, 1419. (c) Li, M. X.; Sun, Q. Z.; Bai, Y.; Duan, C. Y.; Zhang, B. G.; Meng, Q. J. *Dalton Trans* **2006**, 2572. (d) Sun, Q. Z.; Bai, Y.; He, G. J.; Guan, C. Y.; Lin, Z. H.; Meng, Q. J. *Chem. Commun.* **2006**, 2777.

(9) (a) Xiao, D. R.; Wang, E. B.; An, H. Y.; Li, Y. G.; Xu, L. *Cryst. Growth Des.* **2007**, *7*, 506. (b) Huang, X. C.; Li, D.; Chen, X. M. *CrystEngComm* **2006**, *8*, 351. (c) Zhou, J.; Bian, G. Q.; Dai, J.; Zhang, Y.; Zhu, Q. Y.; Lu, W. *Inorg. Chem.* **2006**, *45*, 8486. (d) Cordes, D. B.; Hanton, L. R.; Spicer, M. D. *Inorg. Chem.* **2006**, *45*, 7651. (e) Li, F.; Li, T. H.; Li, X. J.; Li, X.; Wang, Y. L.; Cao, R. *Cryst. Growth Des.* **2006**, *6*, 1458. (f) Luan, X. J.; Wang, Y. Y.; Li, D. S.; Liu, P.; Hu, H. M.; Shi, Q. Z.; Peng, S. M. *Angew. Chem., Int. Ed.* **2005**, *44*, 3864. (g) Yi, L.; Yang, X.; Lu, T. B.; Cheng, P. *Cryst. Growth Des.* **2005**, *5*, 1215. (h) Li, J. R.; Bu, X. H.; Jiao, J.; Du, W. P.; Xu, X. H.; Zhang, R. H. *J. Chem. Soc., Dalton Trans.* **2005**, 464. (i) Li, J. R.; Bu, X. H.; Zhang, R. H. *Eur. J. Inorg. Chem.* **2004**, 1701. (j) Albrecht, M. *Chem. Rev.* **2001**, *101*, 3457.

(10) (a) Han, L.; Hong, M. C. *Inorg. Chem. Commun.* **2005**, *8*, 406, and references therein. (b) Chen, X. Y.; Shi, W.; Xia, J.; Cheng, P.; Zhao, B.; Song, H. B.; Wang, H. G.; Yan, S. P.; Liao, D. Z.; Jiang, Z. H. *Inorg. Chem.* **2005**, *44*, 4263. (c) Siemeling, U.; Schepplmann, I.; Neumann, B.; Stammeler, A.; Stammeler, H.-G.; Frelek, J. *Chem. Commun.* **2003**, 2236. (d) Pérez-García, L.; Amabilino, D. B. *Chem. Soc. Rev.* **2002**, *31*, 342. (e) Biradha, K.; Seward, C.; Zaworotko, M. J. *Angew. Chem., Int. Ed.* **1999**, *38*, 492.

(11) (a) Lu, W. G.; Gu, J. Z.; Jiang, L.; Tan, M. Y.; Lu, T. B. *Cryst. Growth Des.* **2008**, *8*(1), 192–199. (b) Han, L.; Valle, H.; Bu, X. H. *Inorg. Chem.* **2007**, *46*, 1511. (c) Ezuhara, T.; Endo, K.; Aoyama, Y. *J. Am. Chem. Soc.* **1999**, *121*, 3279.

(12) Pasteur, L. *Ann. Chim. Phys.* **1848**, *24*, 442.

(13) (a) Khatua, S.; Stoeckli-Evans, H.; Harada, T.; Kuroda, R.; Bhattacharjee, M. *Inorg. Chem.* **2006**, *45*, 9619. (b) Lonnon, D. G.; Colbran, S. B.; Craig, D. C. *Eur. J. Inorg. Chem.* **2006**, 1190. (c) Telfer, S. G.; Kuroda, R. *Chem.—Eur. J.* **2005**, *11*, 57. (d) Telfer, S. G.; Sato, T.; Kuroda, R. *Angew. Chem., Int. Ed.* **2004**, *43*, 581.

well as the 1D hydrogen bonded zigzag chain of  $\{[\text{Ni}(f\text{-SS-L})(d\text{-Phe})](\text{ClO}_4)_n\}$ . The results exhibit how the different chirality of building blocks affects the helicity of 1D chains.

**Experimental Section**

**Materials and General Methods.** The macrocyclic ligand (L) and its nickel(II) complex were prepared according to the literature method,<sup>1,3</sup> and separated as the racemic form of *rac-L*. The nickel(II) complex  $[\text{Ni}(\alpha\text{-rac-L})](\text{ClO}_4)_2$  was prepared according to the previously reported methods.<sup>4</sup> All of the other chemicals are commercially available and used without further purification. Elemental analyses were determined using Elementar Vario EL elemental analyzer. The IR spectra were recorded in the 4000 to 400  $\text{cm}^{-1}$  region using KBr pellets and a Bruker EQUINOX 55 spectrometer. The solid and solution UV-vis spectra were recorded on a Shimadzu UV-3150 spectrophotometer. The solid (KBr pellets) and solution (in acetonitrile) circular dichroism (CD) spectra were recorded on a JASCO J-810 spectropolarimeter.

**Caution!** Perchlorate salts of metal complexes with organic ligands are potentially explosive. They should be handled with care and prepared only in small quantities.

$\{[\text{Ni}(f\text{-SS-L})(l\text{-Phe})](\text{ClO}_4)_n\}$  ( **$\Delta$ -1**) and  $\{[\text{Ni}_3(f\text{-RR-L})_3(l\text{-Phe})_2](\text{ClO}_4)_4\}_n$  ( **$a$ -2**). A solution of  $[\text{Ni}(\alpha\text{-rac-L})](\text{ClO}_4)_2$  (54 mg, 0.1 mmol) in acetonitrile (5 mL) was added to a solution of *l*-phenylalanine (*l*-HPhe, 16 mg, 0.1 mmol) and NaOH (4 mg, 0.1 mmol) in minimum amount of water. The resultant blue solution was evaporated slowly at room temperature. After two days, violet prism-shaped crystals of  **$\Delta$ -1** were obtained. Yield: 23 mg, 37%. The remaining solution was filtered and evaporated slowly at room temperature. Blue prism-shaped crystals of  **$a$ -2** were isolated after three days, the small amount of impurity of  **$\Delta$ -1** was separated manually ( **$\Delta$ -1** and  **$a$ -2** are easy to distinguish by color). Yield: 21 mg, 24%. Anal. Calcd for  $\text{C}_{25}\text{H}_{47}\text{N}_5\text{ClO}_{6.5}\text{Ni}$  ( **$\Delta$ -1**•0.5H<sub>2</sub>O): C, 48.76; H, 7.69; N, 11.37. Found: C, 48.93; H, 7.82; N, 11.37. IR (KBr): 3422 (s), 3337 (m), 3189 (s), 2970 (m), 2931 (m), 1597 (vs), 1457 (w), 1406 (w), 1167 (m), 1121 (vs), 1082 (m), 989 (w), 756 (w), 707 (m), 624 (m)  $\text{cm}^{-1}$ . Anal. Calc. for  $\text{C}_{66}\text{H}_{130}\text{N}_{14}\text{Cl}_4\text{O}_{21}\text{Ni}_3$  ( **$a$ -2**): C, 44.69; H, 7.38; N, 11.05. Found: C, 44.78; H, 7.51; N, 11.13. IR (KBr): 3514(m), 3337(w), 3256(s), 2974(m), 2936(m), 1607(vs), 1451(w), 1410(w), 1168 (m), 1109 (vs), 972(w), 819(m), 759(m), 708(m), 624(s)  $\text{cm}^{-1}$ .

$\{[\text{Ni}(f\text{-RR-L})(d\text{-Phe})](\text{ClO}_4)_n\}$  ( **$\Lambda$ -1**) and  $\{[\text{Ni}_3(f\text{-SS-L})_3(d\text{-Phe})_2](\text{ClO}_4)_4\}_n$  ( **$b$ -2**). Use of *d*-phenylalanine (*d*-HPhe) in a procedure analogous to that detailed for the preparations of  **$\Lambda$ -1** and  **$a$ -2** afforded 18 mg (29%) of violet prism-shaped crystals of  **$\Lambda$ -1** and 30 mg (34%) of blue crystals of  **$b$ -2**. Anal. Calcd for  $\text{C}_{25}\text{H}_{46}\text{N}_5\text{ClO}_6\text{Ni}$  ( **$\Lambda$ -1**): C, 49.48; H, 7.64; N, 11.54. Found: C, 49.39; H, 7.37; N, 11.11. IR (KBr): 3429 (s), 3338 (m), 3190 (s), 2971 (m), 2935 (m), 1600 (vs), 1453 (w), 1405 (w), 1168 (m), 1119 (vs), 1087 (m), 986 (w), 756 (w), 707 (m), 624 (m)  $\text{cm}^{-1}$ . Anal. Calc. for  $\text{C}_{66}\text{H}_{130}\text{N}_{14}\text{Cl}_4\text{O}_{21}\text{Ni}_3$  ( **$b$ -2**): C, 44.69; H, 7.38; N, 11.05. Found: C, 44.36; H, 7.53; N, 11.05. IR (KBr): 3513(m), 3337(w), 3256(s), 2974(m), 2936(m), 1607(vs), 1451(w), 1409(w), 1168 (m), 1109 (vs), 973(w), 819(m), 759(m), 708(m), 624(vs)  $\text{cm}^{-1}$ .

**Conglomerate of  $\Delta$ -1 and  $\Lambda$ -1 ( $c$ -1).** Use of *dl*-phenylalanine (*dl*-HPhe) in a procedure analogous to that detailed for the preparation of  **$\Delta$ -1** afforded 35 mg (57%) of violet prism-shaped crystals suitable for X-ray analysis, and no blue crystals of  **$a$ -2** and  **$b$ -2** were found in the solution. Anal. Calcd for  $\text{C}_{25}\text{H}_{46}\text{N}_5\text{ClO}_6\text{Ni}$  ( **$c$ -1**): C, 49.48; H, 7.64; N, 11.54. Found: C, 49.90; H, 7.84; N, 11.46. IR (KBr): 3432 (s), 3337 (m), 3189 (s), 2969 (m), 2930

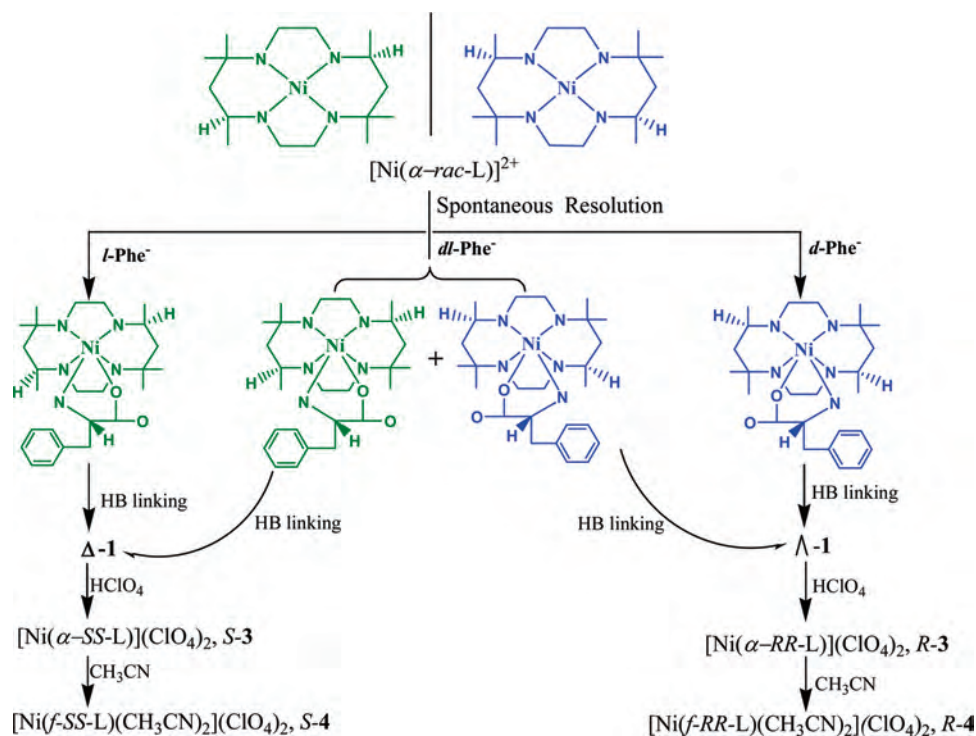
**Table 1.** Crystallographic Data

compound	$\Delta$ -1	$\Lambda$ -1	<b><math>a</math>-2</b>	<b><math>b</math>-2</b>	<b><math>S</math>-4-CH<sub>3</sub>CN</b>	<b><math>R</math>-4-CH<sub>3</sub>CN</b>	<i>rac</i> -4-CH <sub>3</sub> CN	<b><math>5</math>•2CH<sub>3</sub>CN</b>
formula	$\text{C}_{25}\text{H}_{46}\text{ClN}_5\text{NiO}_6$	$\text{C}_{25}\text{H}_{46}\text{ClN}_5\text{NiO}_6$	$\text{C}_{66}\text{H}_{130}\text{Cl}_4\text{N}_{14}\text{Ni}_3\text{O}_{21}$	$\text{C}_{66}\text{H}_{130}\text{Cl}_4\text{N}_{14}\text{Ni}_3\text{O}_{21}$	$\text{C}_{22}\text{H}_{45}\text{Cl}_2\text{N}_7\text{NiO}_8$	$\text{C}_{22}\text{H}_{45}\text{Cl}_2\text{N}_7\text{NiO}_8$	$\text{C}_{22}\text{H}_{45}\text{Cl}_2\text{N}_7\text{NiO}_8$	$\text{C}_{29}\text{H}_{52}\text{ClN}_7\text{NiO}_6$
fw	606.83	606.83	1773.77	1773.77	665.26	665.26	665.26	688.94
temperature (K)	173(2)	173(2)	173(2)	173(2)	173(2)	173(2)	173(2)	173(2)
crystal size (mm)	$0.42 \times 0.18 \times 0.14$	$0.48 \times 0.25 \times 0.22$	$0.45 \times 0.25 \times 0.22$	$0.45 \times 0.20 \times 0.13$	$0.42 \times 0.26 \times 0.23$	$0.48 \times 0.47 \times 0.42$	$0.48 \times 0.32 \times 0.27$	$0.45 \times 0.42 \times 0.21$
crystal system	tetragonal	tetragonal	orthorhombic	orthorhombic	orthorhombic	orthorhombic	orthorhombic	monoclinic
space group	$P4_1$	$P4_3$	$P2_12_12_1$	$P2_12_12_1$	$P2_12_12_1$	$P2_12_12_1$	$P2_12_12_1$	$P2_1$
<i>a</i> /Å	12.6088(11)	12.6159(9)	14.993(3)	15.0034(19)	9.2987(11)	9.293(2)	9.3344(16)	9.5072(17)
<i>b</i> /Å	12.6088(11)	12.6159(9)	18.324(4)	18.362(2)	14.2949(18)	14.314(4)	14.565(3)	14.552(3)
<i>c</i> /Å	18.180(3)	18.211(3)	30.432(6)	30.475(4)	23.931(3)	23.964(7)	23.970(4)	12.861(2)
$\beta$ /deg	90	90	90	90	90	90	90	101.089(3)
volume /Å <sup>3</sup>	2890.3(6)	2898.4(5)	8361(3)	8395.7(18)	3181.0(7)	3187.7(14)	3258.9(10)	1746.0(6)
Z	4	4	4	4	4	4	4	2
<i>D</i> <sub>x</sub> /g cm <sup>-3</sup>	1.395	1.391	1.409	1.403	1.389	1.386	1.356	1.310
$\mu$ /mm <sup>-1</sup>	0.811	0.808	0.872	0.868	0.830	0.829	0.811	0.681
unique refl. ( <i>R</i> <sub>int</sub> )	5982 (0.0518)	6142 (0.0337)	17994 (0.0890)	18165 (0.0865)	6921 (0.0494)	6566 (0.0336)	6385 (0.0733)	7474 (0.0268)
parameters	349	349	974	974	370	370	417	399
<i>S</i> on <i>F</i> <sup>2</sup>	1.015	1.027	0.959	1.033	1.008	1.045	0.935	1.007
<i>R</i> <sub>1</sub> , <sup>a</sup> <i>wR</i> <sub>2</sub> <sup>b</sup> ( <i>I</i> > 2σ( <i>I</i> ))	0.0456, 0.0931	0.0375, 0.0792	0.0590, 0.1164	0.0695, 0.1403	0.0461, 0.0858	0.0439, 0.0873	0.0578, 0.1199	0.0376, 0.0845
<i>R</i> <sub>1</sub> , <sup>a</sup> <i>wR</i> <sub>2</sub> <sup>b</sup> (all data)	0.0795, 0.1055	0.0567, 0.0868	0.1252, 0.1387	0.1423, 0.1716	0.0881, 0.0995	0.0745, 0.1003	0.1510, 0.1550	0.0513, 0.0906
absolute structure parameter	0.001(15)	0.003(12)	-0.026(13)	-0.019(15)	-0.002(17)	0.007(17)	0.48(3)	0.023(11)

<sup>a</sup> *R*<sub>1</sub> = Σ|*F*<sub>o</sub> - |*F*<sub>c</sub>||/Σ|*F*<sub>o</sub>||, <sup>b</sup> *wR*<sub>2</sub> = [Σ(*w*(*F*<sub>o</sub> - |*F*<sub>c</sub>||)<sup>2</sup>)/Σ(*w*(*F*<sub>o</sub>)<sup>2</sup>)]<sup>1/2</sup>, *w* = 1/[σ<sup>2</sup>(*F*<sub>o</sub>)<sup>2</sup> + (*aP*)<sup>2</sup> + *bP*], where *P* = [(*F*<sub>o</sub>)<sup>3</sup> + 2*F*<sub>c</sub><sup>2</sup>]/3.



## Scheme 2



(m), 1598 (vs), 1456 (w), 1405 (w), 1167 (m), 1120 (vs), 1087 (m), 989 (w), 756 (w), 707 (m), 624 (m)  $\text{cm}^{-1}$ .

**$[\text{Ni}(\alpha\text{-SS-L})](\text{ClO}_4)_2$  (S-3) and  $[\text{Ni}(\alpha\text{-RR-L})](\text{ClO}_4)_2$  (R-3).** The crystals of  $\Delta\text{-1}$  or  $\Lambda\text{-1}$  were immersed in an aqueous solution of perchloric acid (48%) until the color changed from violet to yellow. The yellow solid was filtered, washed with water and dried under vacuum. Anal. Calcd for  $\text{C}_{16}\text{H}_{37.5}\text{N}_4\text{Cl}_{3.5}\text{O}_{14}\text{Ni}$  (S-3 $\cdot$ 1.5HClO<sub>4</sub>): C, 27.74; H, 5.46; N, 8.09. Found: C, 27.96; H, 5.63; N, 7.63.; IR (KBr): 3205 (w), 3095 (m), 2974 (m), 2921 (w), 1741 (w), 1459 (w), 1379 (m), 1279 (w), 1145 (s), 1111 (s), 1085 (s), 819 (w), 776 (w), 627 (vs)  $\text{cm}^{-1}$ . Anal. Calcd for  $\text{C}_{16}\text{H}_{37.7}\text{N}_4\text{Cl}_{3.7}\text{O}_{14.8}\text{Ni}$  (R-

3 $\cdot$ 1.7HClO<sub>4</sub>): C, 26.96; H, 5.33; N, 7.86. Found: C, 27.05; H, 5.58; N, 7.49. IR (KBr): 3206 (w), 3095 (m), 2971 (m), 2874 (w), 1740 (w), 1459 (w), 1378 (m), 1278 (w), 1146 (s), 1113 (s), 1088 (s), 820 (w), 776 (w), 627 (vs)  $\text{cm}^{-1}$ .

**$[\text{Ni}(f\text{-SS-L})(\text{CH}_3\text{CN})_2](\text{ClO}_4)_2$  (S-4),  $[\text{Ni}(f\text{-RR-L})(\text{CH}_3\text{CN})_2](\text{ClO}_4)_2$  (R-4), and  $[\text{Ni}(f\text{-rac-L})(\text{CH}_3\text{CN})_2](\text{ClO}_4)_2$  (rac-4).** The yellow powder of S-3/R-3 or  $[\text{Ni}(\alpha\text{-rac-L})](\text{ClO}_4)_2$  was dissolved in  $\text{CH}_3\text{CN}$ . The resulting purple solution was evaporated slowly at room temperature to give purple prism-shaped crystals. Yield: 85% for S-4 $\cdot$ CH<sub>3</sub>CN, 81% for R-4 $\cdot$ CH<sub>3</sub>CN and 87% for rac-4 $\cdot$ CH<sub>3</sub>CN. Anal. Calcd for  $\text{C}_{22}\text{H}_{47}\text{N}_7\text{Cl}_2\text{O}_9\text{Ni}$  (S-4 $\cdot$ CH<sub>3</sub>CN $\cdot$ H<sub>2</sub>O): C, 38.67; H, 6.93; N, 14.35. Found: C, 38.98; H, 7.02; N, 14.51. IR (KBr): 3585 (m), 3449 (m), 3207 (s), 2975 (m), 2884 (w), 2282 (w), 2250 (w), 2021 (w), 1614 (w), 1460 (s), 1379 (s), 1275 (w), 1087 (vs), 1008 (w), 819 (m), 777 (w), 625 (vs)  $\text{cm}^{-1}$ . Anal. Calcd for  $\text{C}_{22}\text{H}_{47}\text{N}_7\text{Cl}_2\text{O}_9\text{Ni}$  (R-4 $\cdot$ CH<sub>3</sub>CN $\cdot$ H<sub>2</sub>O): C, 38.67; H, 6.93; N, 14.35. Found: C, 38.78; H, 6.92; N, 14.11. IR (KBr): 3578 (m), 3450 (m), 3207 (s), 2972 (m), 2875 (w), 2285 (w), 2252 (w), 2023 (w), 1631 (w), 1459 (s), 1379 (s), 1276 (w), 1087 (vs), 1008 (w), 820 (m), 777 (w), 627 (vs)  $\text{cm}^{-1}$ . Anal. Calcd for  $\text{C}_{22}\text{H}_{45}\text{N}_7\text{Cl}_2\text{O}_8\text{Ni}$  (rac-4 $\cdot$ CH<sub>3</sub>CN): C, 39.72; H, 6.82; N, 14.74. Found: C, 39.38.; H, 7.02; N, 14.58. IR (KBr): 3458 (w), 3257 (s), 3027 (w), 2971 (m), 2876 (w), 2283 (w), 2251 (w), 2020 (w), 1460 (s), 1372 (s), 1275 (w), 1096 (vs), 1040 (w), 976 (s), 820 (m), 777 (w), 626 (vs)  $\text{cm}^{-1}$ .

**$\{[\text{Ni}(f\text{-SS-L})(d\text{-Phe})](\text{ClO}_4)\}_n$  (5).** A solution of S-3 (54 mg, 0.1 mmol) in acetonitrile (5 mL) was added to a solution of *d*-HPhe (16 mg, 0.1 mmol) and NaOH (4 mg, 0.1 mmol) in minimum amount of water. The mixture was evaporated slowly at room temperature to give blue prism-shaped crystals of 5 $\cdot$ 2CH<sub>3</sub>CN. Yield: 39 mg, 63%. Anal. Calc. for  $\text{C}_{25}\text{H}_{46}\text{N}_5\text{ClO}_6\text{Ni}$  (5): C, 49.48; H, 7.64; N, 11.54. Found: C, 49.21; H, 7.51; N, 11.34. IR (KBr): 3514(m), 3337(w), 3255(s), 2975(m), 2936(m), 2030(w), 1607(vs), 1454(w), 1411(w), 1168 (m), 1110 (vs), 972(w), 819(m), 759(m), 708(m), 623(vs)  $\text{cm}^{-1}$ .

**X-Ray Crystallography.** Single-crystal data for  $\Delta\text{-1}$ ,  $\Lambda\text{-1}$ , *a*-2, *b*-2, S-4 $\cdot$ CH<sub>3</sub>CN, R-4 $\cdot$ CH<sub>3</sub>CN, rac-4 $\cdot$ CH<sub>3</sub>CN, and 5 $\cdot$ 2CH<sub>3</sub>CN

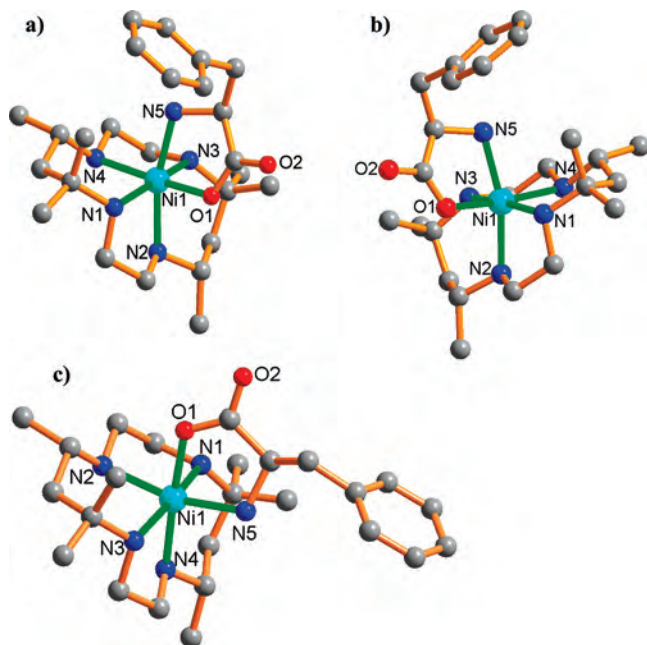


**Figure 1.** Enantiomers of (a)  $[\text{Ni}(f\text{-SS-L})(L\text{-Phe})]^+$  in  $\Delta\text{-1}$  and (b)  $[\text{Ni}(f\text{-RR-L})(d\text{-Phe})]^+$  in  $\Lambda\text{-1}$ . (c) Diastereomer of  $[\text{Ni}(f\text{-SS-L})(d\text{-Phe})]^+$  in 5.

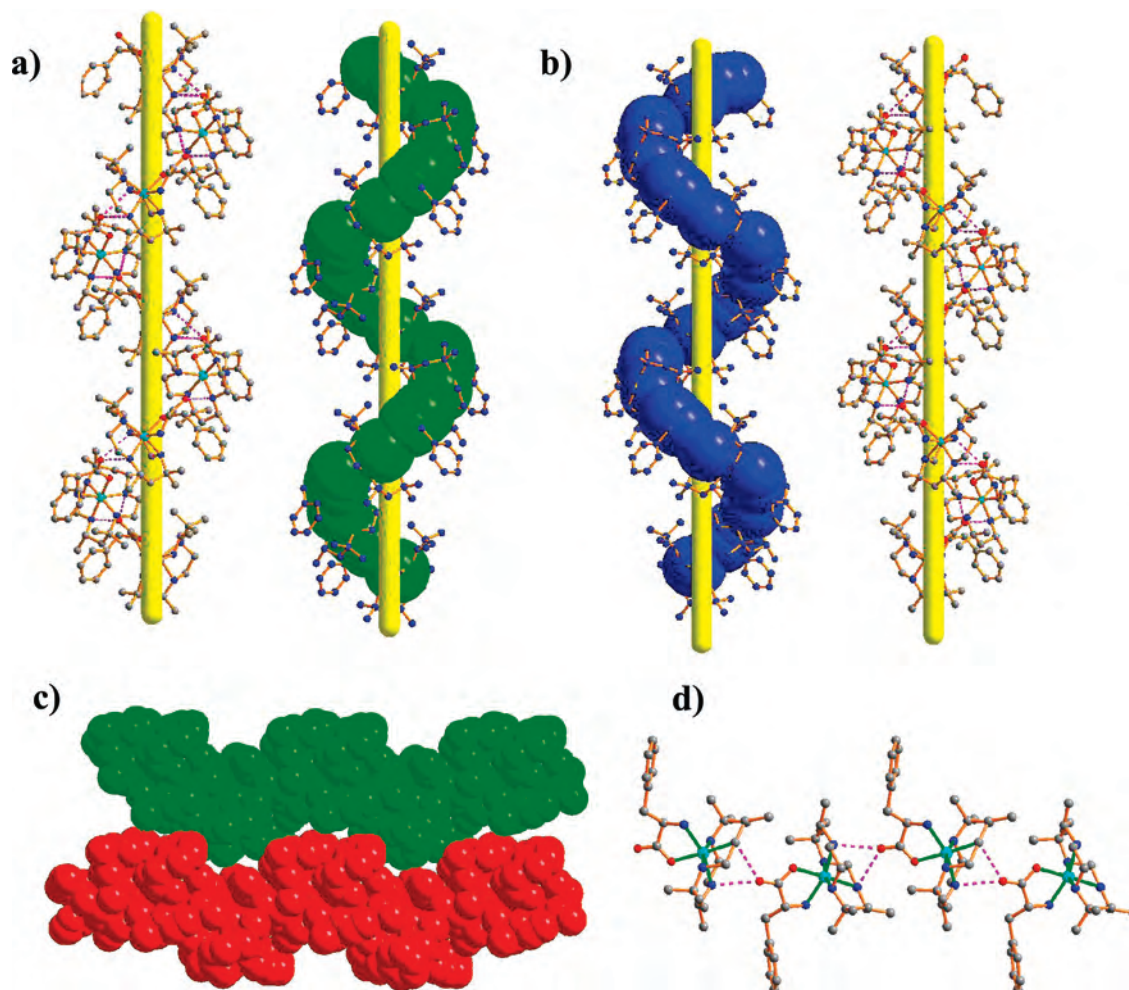


**Figure 2.** Side view of (a) 1D hydrogen bonded right-handed helical chain in  $\Delta$ -1 and (b) 1D hydrogen bonded left-handed helical chain in  $\Lambda$ -1. (c) Space filling mode for two adjacent helical chains in  $\Delta$ -1, showing the homochirality transfer through the interchain zipperlike complementary hydrophobic interactions. (d) 1D hydrogen bonded zigzag chain in **5**.

were collected on a Bruker Smart 1000 CCD diffractometer, with Mo K $\alpha$  radiation ( $\lambda = 0.71073$  Å). All empirical absorption corrections were applied using the SADABS program.<sup>14</sup> The structures were solved using direct methods, which yielded the positions of all nonhydrogen atoms. These were refined first isotropically and then anisotropically. All the hydrogen atoms of the ligands were placed in calculated positions with fixed isotropic thermal parameters and included in the structure factor calculations in the final stage of full-matrix least-squares refinement. All calculations were performed using the SHELXTL system of computer programs.<sup>15</sup> The crystallographic data for  $\Delta$ -1,  $\Lambda$ -1, *a*-2, *b*-2, *S*-4 $\cdot$ CH<sub>3</sub>CN, *R*-4 $\cdot$ CH<sub>3</sub>CN, *rac*-4 $\cdot$ CH<sub>3</sub>CN, and **5** $\cdot$ 2CH<sub>3</sub>CN are summarized in Table 1. The selected bond lengths and angles are listed in Table S1 (see the Supporting Information).

## Results and Discussion

**Preparation Chemistry.** It has been reported that the racemic [Ni( $\alpha$ -*rac*-L)](ClO<sub>4</sub>)<sub>2</sub> can be separated to two enantiomers through its *l*- or *d*-tartrato-nickel(II) complex,

followed by removing tartrate using perchloric acid.<sup>16</sup> Since  $\alpha$ -isomer [Ni( $\alpha$ -*rac*-L)]<sup>2+</sup> is easy to isomerize to the thermodynamically more stable  $\beta$ -isomer [Ni( $\beta$ -*rac*-L)]<sup>2+</sup> in neutral and basic media,<sup>1</sup> it is necessary to convert the perchlorate salt to the bromide salt prior to reaction with tartrate, so as to enhance the solubility and to dissolve quickly the racemic compound in the  $\alpha$ -form in water.<sup>16a</sup>

In this paper, we demonstrated that phenylalanine are also effective for optical resolution of [Ni( $\alpha$ -*rac*-L)](ClO<sub>4</sub>)<sub>2</sub>. We found that the stability and solubility of  $\alpha$ -isomer in water are increased by adding acetonitrile, so [Ni( $\alpha$ -*rac*-L)](ClO<sub>4</sub>)<sub>2</sub> need not convert to bromide salt, and can directly react with *l*- and *d*-Phe<sup>-</sup> to generate two less-soluble enantiomers of  $\Delta$ -1 and  $\Lambda$ -1, respectively. The remaining solutions were evaporated at room temperature to give two diastereomers of *a*-2 and *b*-2. The reaction of [Ni( $\alpha$ -*rac*-L)](ClO<sub>4</sub>)<sub>2</sub> with racemic *dl*-Phe<sup>-</sup> gave a conglomerate of *c*-1; in which *SS* and *RR* enantiomers in [Ni( $\alpha$ -*rac*-L)]<sup>2+</sup> preferentially coordinate to *l*- and *d*-Phe<sup>-</sup>, respectively, generating a racemic mixture of  $\Delta$ -1 and  $\Lambda$ -1. Spontaneous resolution occurred

(14) Sheldrick, G. M. *SADABS, Program for Empirical Absorption Correction of Area Detector Data*; University of Göttingen: Göttingen, 1996.

(15) Sheldrick, G. M. *SHELXS 97, Program for Crystal Structure Refinement*; University of Göttingen: Göttingen, 1997.

(16) (a) Ito, H.; Fujita, J.; Toriumi, K.; Ito, T. *Bull. Chem. Soc. Jpn.* **1981**, *54*, 2988. (b) Bryan, P. S.; Dabrowiak, J. C. *Inorg. Chem.* **1975**, *14*, 299.



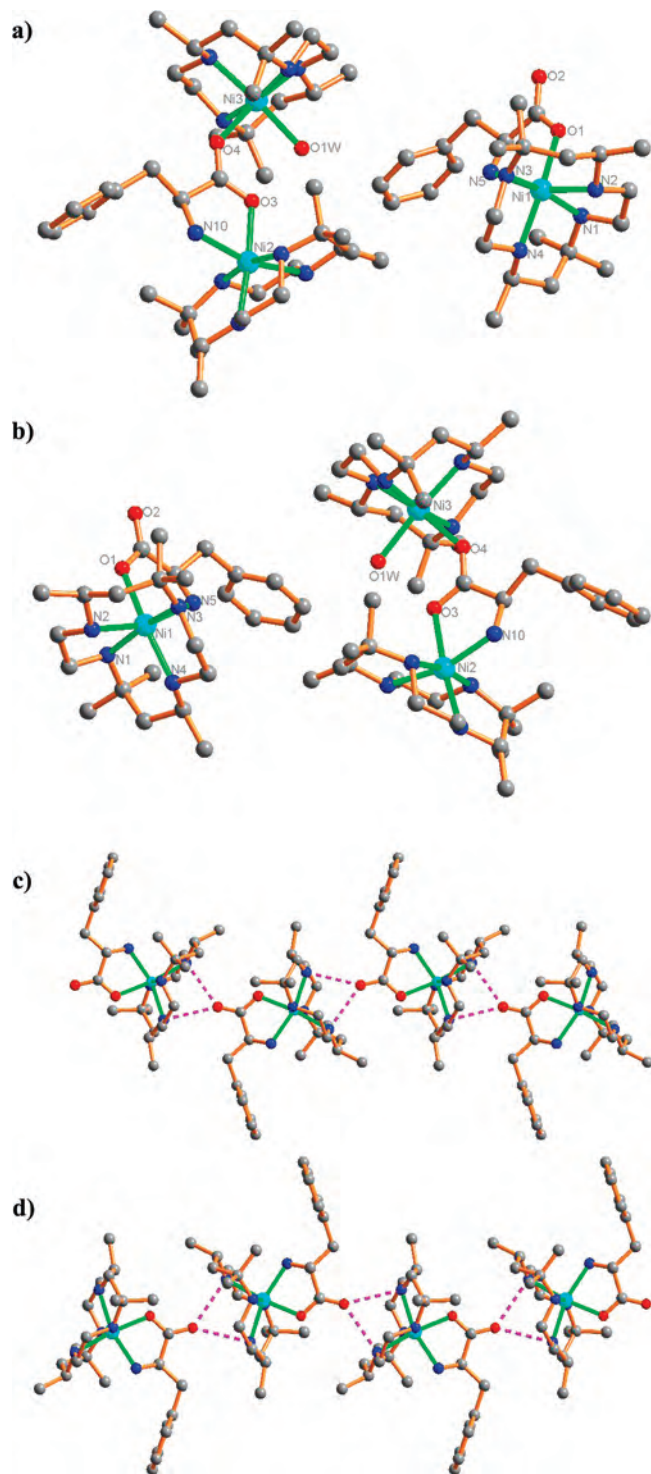


**Figure 3.** Structural cations of (a)  $[\text{Ni}_3(f\text{-}RR\text{-}L)_3(l\text{-}Phe)_2]^{4+}$  in *a-2* and (b)  $[\text{Ni}_3(f\text{-}SS\text{-}L)_3(d\text{-}Phe)_2]^{4+}$  in *b-2* and the side view of 1D hydrogen bonded zigzag chains of (c)  $[\text{Ni}(f\text{-}RR\text{-}L)(l\text{-}Phe)]_n^{4+}$  in *a-2* and (d)  $[\text{Ni}(f\text{-}SS\text{-}L)(d\text{-}Phe)]_n^{4+}$  in *b-2*.

during the reaction, in which each crystal crystallized into enantiopure. Removing phenylalanine in  $\Delta\text{-1}$  and  $\Lambda\text{-1}$  using perchloric acid yielded two enantiomers of  $[\text{Ni}(\alpha\text{-}SS\text{-}L)(\text{ClO}_4)_2]$  (*S-3*) and  $[\text{Ni}(\alpha\text{-}RR\text{-}L)(\text{ClO}_4)_2]$  (*R-3*), respectively. The *SS* and *RR* enantiomers were dissolved in acetonitrile to generate two enantiomers of  $[\text{Ni}(f\text{-}SS\text{-}L)(\text{CH}_3\text{CN})_2](\text{ClO}_4)_2$  (*S-4*) and  $[\text{Ni}(f\text{-}RR\text{-}L)(\text{CH}_3\text{CN})_2](\text{ClO}_4)_2$  (*R-4*), respectively (see Scheme 2).

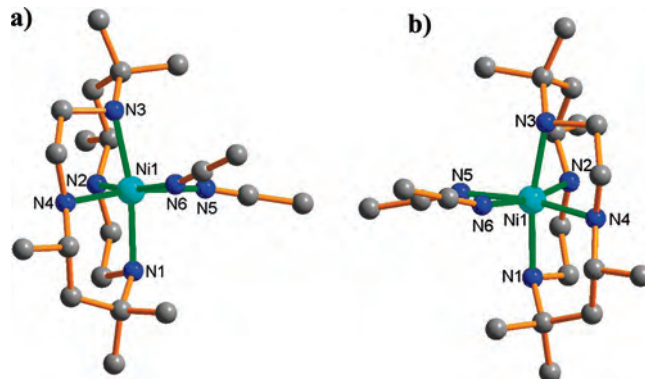


**Figure 4.** Enantiomers of (a) *S-4* and (b) *R-4*.

**Crystal Structures of  $\Delta\text{-1}$ ,  $\Lambda\text{-1}$ , and **5**.** One asymmetric unit in  $\Delta\text{-1}$ ,  $\Lambda\text{-1}$ , and **5** contains one  $[\text{Ni}(f\text{-}SS\text{-}L)(l\text{-}Phe)]^+$ ,  $[\text{Ni}(f\text{-}RR\text{-}L)(d\text{-}Phe)]^+$  and  $[\text{Ni}(f\text{-}SS\text{-}L)(d\text{-}Phe)]^+$ , respectively, and one  $\text{ClO}_4^-$ .  $[\text{Ni}(f\text{-}SS\text{-}L)(l\text{-}Phe)]^+$  and  $[\text{Ni}(f\text{-}RR\text{-}L)(d\text{-}Phe)]^+$  are enantiomer (Figure 1a and b). In each cation (Figure 1), the nickel(II) ion displays a distorted octahedral coordination geometry by coordination with four nitrogen atoms of L in a folded conformation, and one carboxylate oxygen atom and one nitrogen atom of *l*- or *d*- $\text{Phe}^-$  in *cis*-position. The macrocyclic ligand L adopts a *SS*, *RR* and *SS* configuration in  $\Delta\text{-1}$ ,  $\Lambda\text{-1}$ , and **5**, respectively (Figure 1). In each compound, the Ni–O distance is shorter than the Ni–N distances (see Table S1). In  $\Delta\text{-1}$ , the  $[\text{Ni}(f\text{-}SS\text{-}L)(l\text{-}Phe)]^+$  monomers are connected through the hydrogen bonds between uncoordinated carboxylate oxygen atom of *l*- $\text{Phe}^-$  and two secondary amines of L of adjacent  $[\text{Ni}(f\text{-}SS\text{-}L)(l\text{-}Phe)]^+$  cation, generating a novel 1D right-handed homochiral helical chain along the  $4_1$  axis (Figure 2a). Each helix in the chain contains four  $[\text{Ni}(f\text{-}SS\text{-}L)(l\text{-}Phe)]^+$  monomers, with the pitch of 18.18 Å. The right-handed chirality of the original helical chain is transferred uniformly to adjacent chains through the zipperlike interchain hydrophobic interactions (Figure 2c),<sup>6</sup> resulting in the formation of a supramolecular stereoisomer of  $\Delta\text{-1}$ , with a chiral space group  $P4_1$  and absolute structure parameter of 0.001(15).

In contrast to  $\Delta\text{-1}$ , a 1D left-handed homochiral helical chain is generated by the connections of corresponding  $[\text{Ni}(f\text{-}RR\text{-}L)(d\text{-}Phe)]^+$  enantiomers in  $\Lambda\text{-1}$  through the same intermolecular hydrogen bonds (Figure 2b). Obviously, the *left*-handedness originates from the opposite chirality of *RR*-L and *d*- $\text{Phe}^-$ , and the corresponding supramolecular stereoisomer of  $\Lambda\text{-1}$  is formed through the zipperlike interchain hydrophobic interactions of 1D left-handed helical chains along the  $4_3$  axis, with the opposite chiral space group of  $P4_3$  and absolute structure parameter of 0.003(12).

In **5**, the coordination of  $[\text{Ni}(f\text{-}SS\text{-}L)]^{2+}$  with *d*- $\text{Phe}^-$  gives a diastereomer of  $[\text{Ni}(f\text{-}SS\text{-}L)(d\text{-}Phe)]^+$ , in which the coordination geometry of Ni(II) and the bond distances and angles around Ni(II) are similar to those in  $\Delta\text{-1}$  and  $\Lambda\text{-1}$  (Figure 1c and Table S1). However, the connections of  $[\text{Ni}(f\text{-}SS\text{-}L)(d\text{-}Phe)]^+$  monomers through the same intermolecular hydrogen bonds as  $\Delta\text{-1}$  and  $\Lambda\text{-1}$  generate a 1D zigzag chain instead of 1D helical chain (Figure 2d). This demonstrates that the helicity of a 1D chain is much affected by the

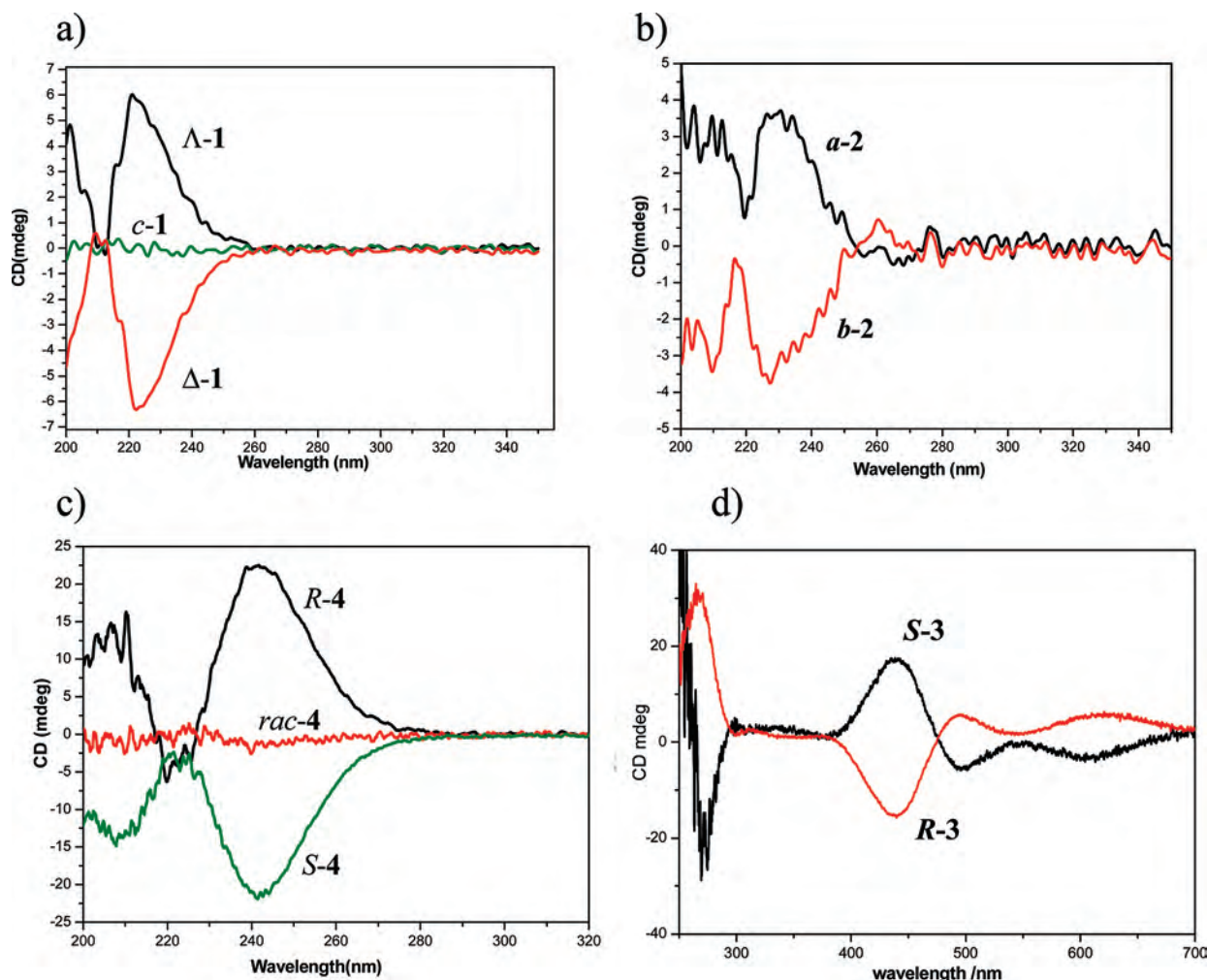


**Figure 5.** CD spectra of (a)  $\Delta$ -1,  $\Lambda$ -1, and *c*-1, (b) *a*-2 and *b*-2, (c) *S*-4, *R*-4, and *rac*-4 in acetonitrile. (d) Solid CD. spectra of *S*-3 and *R*-3.

chirality of its building blocks, i.e. only the binding of  $[\text{Ni}(f\text{-SS-L})]^{2+}$  with *l*-Phe<sup>-</sup> can generate the 1D right-handed helical chain, while the binding of  $[\text{Ni}(f\text{-SS-L})]^{2+}$  with *d*-Phe<sup>-</sup> leads to the formation of 1D zigzag chain. These structural features are very similar to those of peptides. It has been found that the *right*-handedness of peptides originates from the connections of *l*-amino acids, and a peptide with left-handed helix was constructed using corresponding *d*-amino acids as building blocks.<sup>17</sup> In addition, the connections of alternating *l*- and *d*-amino acids in cyclic peptides generated zigzag  $\beta$ -sheets instead of  $\infty$ -helical peptides.<sup>18</sup> In addition, there are acetonitrile molecules between the adjacent zigzag chains in **5** (Figure S1a in the Supporting Information), while no solvents are involved in  $\Delta$ -1 and  $\Lambda$ -1 since there are no voids between the helical chains due to the tight zipperlike interchain hydrophobic interactions (Figure S1b). In comparison to zigzag arrangements in **5**, the zipperlike interchain hydrophobic interactions between helical chains make the accumulations in  $\Delta$ -1 and  $\Lambda$ -1 more compact, and the volume per formula unit of  $\Delta$ -1 or  $\Lambda$ -1 is  $150.5 \text{ \AA}^3$  smaller than that

of **5** (see Table 1). Therefore, in comparison to **5**, the lower solubility of  $\Delta$ -1 and  $\Lambda$ -1 can be attributed to the compact zipperlike interchain packing, so  $\Delta$ -1 and  $\Lambda$ -1 were first isolated from the reaction mixture of  $[\text{Ni}(\alpha\text{-rac-L})](\text{ClO}_4)_2$  and *l*-Phe<sup>-</sup>/*d*-Phe<sup>-</sup>, respectively.

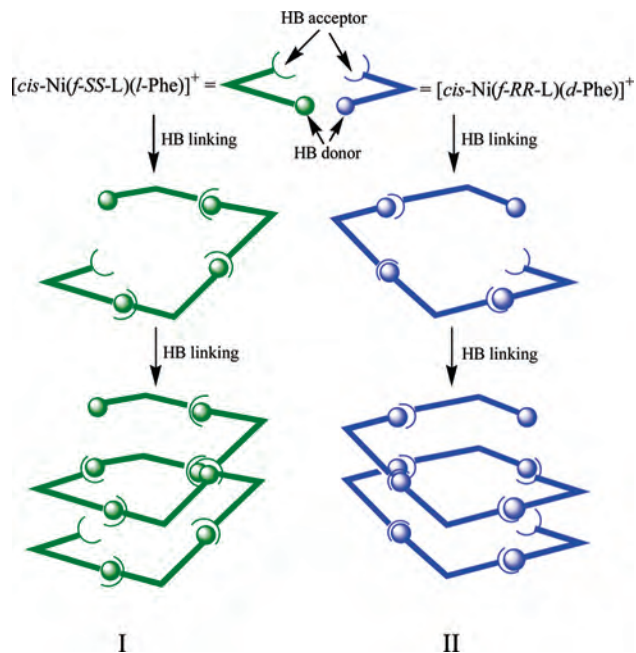
It is interesting to note that spontaneous resolution occurred during the reaction of  $[\text{Ni}(\alpha\text{-rac-L})](\text{ClO}_4)_2$  with *dl*-Phe<sup>-</sup>, giving a conglomerate of *c*-1 (a racemic mixture of  $\Delta$ -1 and  $\Lambda$ -1), in which each crystal crystallized into enantiopure  $\Delta$ -1 or  $\Lambda$ -1, and no crystals of *a*-2 and *b*-2 are isolated from the solution. During this process, *l*-Phe<sup>-</sup> and *d*-Phe<sup>-</sup> preferentially bind  $[\text{Ni}(\alpha\text{-SS-L})]^{2+}$  and  $[\text{Ni}(\alpha\text{-RR-L})]^{2+}$ , respectively, generating two enantiomers of  $[\text{Ni}(f\text{-SS-L})(l\text{-Phe})]^+$  and  $[\text{Ni}(f\text{-RR-L})(d\text{-Phe})]^+$ . The stereoeffect of chiral *f*-SS-L and *l*-Phe<sup>-</sup> in  $[\text{Ni}(f\text{-SS-L})(l\text{-Phe})]^+$  generates a stereoselective environment that only  $[\text{Ni}(f\text{-SS-L})(l\text{-Phe})]^+$  monomers can be congregated along the  $4_1$  helical axis via intermolecular hydrogen bonds (Figure S2a in the Supporting Information). Thus, all  $[\text{Ni}(f\text{-SS-L})(l\text{-Phe})]^+$  monomers are polymerized uniformly along the  $4_1$  axis through the intermolecular hydrogen bonds according to process I (Scheme 3), resulting in a right-handed helical chain, and the helical chains are further aggregated through interchain hydrophobic interactions to isolate an insoluble enantiopure crystal of  $\Delta$ -1 from

(17) Banerjee, A.; Raghothama, S. R.; Karle, I. L.; Balaram, P. *Biopolymers* **1996**, *39*, 279.

(18) (a) Langs, D. A. *Science* **1988**, *241*, 188. (b) Ghadiri, M. R.; Granja, J. R.; Buchler, L. K. *Nature* **1994**, *369*, 301. (c) Clark, T. D.; Ghadiri, M. R. *J. Am. Chem. Soc.* **1995**, *117*, 12364.



**Scheme 3.** Two Different Polymerizing Processes of  $[\text{Ni}(f\text{-SS-L})(l\text{-Phe})]^+$  and  $[\text{Ni}(f\text{-RR-L})(d\text{-Phe})]^+$  through Intermolecular Hydrogen Bonds<sup>a</sup>



<sup>a</sup> HB donor represents the uncoordinated carboxylate oxygen atom of  $\text{Phe}^-$ , and HB acceptor represents the two hydrogen atoms of two secondary amines of L; see Figure S2a and b in the Supporting Information.

solution (Figure 2c). Similarly, the polymerization of  $[\text{Ni}(f\text{-RR-L})(d\text{-Phe})]^+$  monomers according to process II (Scheme 3 and Figure S2b), as well as the aggregation through interchain hydrophobic interactions, generate an enantiopure crystal of  $\Lambda\text{-1}$ , in which all  $[\text{Ni}(f\text{-RR-L})(d\text{-Phe})]^+$  are arranged in a left-handed helix along the  $4_3$  axis. The above results demonstrate that intermolecular hydrogen bonds and hydrophobic interactions play key roles in spontaneous resolution. Based on the above results we can guess that a spontaneous resolution may also occur when *dl*-amino acids are used for the constructions of peptides, giving a racemic mixture of right-handed and left-handed peptides, in which *l*- and *d*-amino acids self-sort and uniformly locate in the right-handed and left-handed peptides, respectively.

**Crystal Structures of *a*-2 and *b*-2.** Both compounds crystallize in the same chiral space group,  $P2_12_12_1$ , with the absolute structure parameters of  $-0.026(13)$  and  $-0.019(15)$ , respectively. In each compound, one asymmetric unit contains one  $\{[\text{Ni}(f\text{-RR-L})_2(l\text{-Phe})]^{3+}/[\text{Ni}(f\text{-SS-L})_2(d\text{-Phe})]^{3+}\}$  dimer, one  $[\text{Ni}(f\text{-RR-L})(l\text{-Phe})]^+ / [\text{Ni}(f\text{-SS-L})(d\text{-Phe})]^+$  cation, and four  $\text{ClO}_4^-$  anions (Figure 3a and b).  $\{[\text{Ni}(f\text{-SS-L})_2(d\text{-Phe})]^{3+}$  and  $\{[\text{Ni}(f\text{-RR-L})_2(l\text{-Phe})]^{3+}$ , as well as  $[\text{Ni}(f\text{-SS-L})(d\text{-Phe})]^+$  and  $[\text{Ni}(f\text{-RR-L})(l\text{-Phe})]^+$ , can be regarded as enantiomers. In *a*-2, two  $[\text{Ni}(f\text{-RR-L})]^{2+}$  are bridged by *l*- $\text{Phe}^-$  to form a dimer of  $\{[\text{Ni}(f\text{-RR-L})_2(l\text{-Phe})]^{3+}$  (Figure 3a), in which each Ni(II) shows a slightly distorted octahedral geometry. The structure of  $[\text{Ni}(f\text{-RR-L})(l\text{-Phe})]^+$  in *a*-2 is the same as that in **5**, with similar octahedral coordination geometry and close bond lengths and angles, and the  $[\text{Ni}(f\text{-RR-L})(l\text{-Phe})]^+$  monomers are also connected by the same intermolecular hydrogen bonds as  $\Delta\text{-1}$ ,  $\Lambda\text{-1}$ , and **5** to form a 1D zigzag chain (Figure 3c). The

$\{[\text{Ni}(f\text{-SS-L})(d\text{-Phe})]^+\}_n$  chains are surrounded and separated by  $\{[\text{Ni}(f\text{-RR-L})_2(l\text{-Phe})]^{3+}\}$  dimers to form a 3D structure of *a*-2 (Figure S3 in the Supporting Information). In comparison to  $\Delta\text{-1}$ , the relative loose packing arrangement in *a*-2 makes *a*-2 more soluble, thus  $\Delta\text{-1}$  and *a*-2 can be separated by crystallization.

Compound *b*-2 shows similar structure and solubility to *a*-2, except the opposite chirality of *f*-SS-L and *d*-Phe<sup>-</sup> in *b*-2 (Figure 3b and d).

**Crystal Structures of *S*-4, *R*-4, and *rac*-4.** All three compounds of *S*-4, *R*-4, and *rac*-4 crystallize in the same chiral space group,  $P2_12_12_1$ , with the absolute structure parameters of  $-0.002(17)$ ,  $0.007(17)$ , and  $0.48(3)$ , respectively, indicating the homochiral nature of *S*-4 and *R*-4, and the crystallization of *rac*-4 is racemic twinning. All three compounds show similar structures, in which each Ni(II) is six-coordinated to four nitrogen atoms of the folded L, and two acetonitrile molecules in *cis* position. The *S*-4 and *R*-4 are a pair of enantiomers (Figure 4), and the configurations of L in *S*-4 and *R*-4 are *SS* and *RR*, respectively.

**UV-vis and CD Spectra.** The solid UV-vis spectra were recorded as the compounds do not show absorption peaks in acetonitrile (except *S*-4 and *R*-4), probably due to the strong absorption of acetonitrile around 220 nm. The solid UV-vis spectra show two absorption peaks at 241 and 366 nm for  $\Delta\text{-1}/\Lambda\text{-1}$ , 216 and 373 nm for *a*-2/*b*-2, and 254 and 452 nm for *S*-3/*R*-3, respectively (Figure S4 in the Supporting Information). Compounds *S*-4/*R*-4 display one absorption peak around 230 nm in acetonitrile (Figure S4). The results of CD measurements confirm the chiral nature of  $\Delta\text{-1}/\Lambda\text{-1}$ , *a*-2/*b*-2, *S*-3/*R*-3, and *S*-4/*R*-4. As shown in Figure 5a, the bulk crystals of  $\Delta\text{-1}$  in acetonitrile show a positive and a negative Cotton effects at 209 and 221 nm, respectively, while the bulk crystals of  $\Delta\text{-1}$  in acetonitrile show opposite Cotton effects at the same wavelengths. There is no visible dichroic signal for the bulk crystals of *c*-1, but each crystal of *c*-1, which was random picked up from the bulk crystals of *c*-1, shows similar dichroic signals to those of  $\Delta\text{-1}$  or  $\Lambda\text{-1}$ , indicating spontaneous resolution occurred during the reaction of  $[\text{Ni}(\alpha\text{-rac-L})](\text{ClO}_4)_2$  with *dl*- $\text{Phe}^-$  to generate a conglomerate of *c*-1. The CD spectra of *a*-2 and *b*-2 in acetonitrile display similar Cotton effects to  $\Delta\text{-1}$  and  $\Lambda\text{-1}$ , respectively (Figure 5b), indicating the displayed Cotton effects are mainly contributed by the chiral macrocyclic ligand. This also indicates that the 1D hydrogen bonded helical chains in  $\Delta\text{-1}$  and  $\Lambda\text{-1}$ , and zigzag chains in *a*-2 and *b*-2, may be decomposed to corresponding monomers or oligomers.

The solid CD spectra of *S*-3 and *R*-3 also show the opposite Cotton effects at  $\lambda = 265, 440, 503,$  and  $636$  nm (Figure 5d), indicating the chirality of L is still preserved after removing phenylalanine, and racemic  $[\text{Ni}(\alpha\text{-rac-L})](\text{ClO}_4)_2$  was successfully separated to two enantiomers of *S*-3 and *R*-3. The CD spectra of *S*-4 and *R*-4 in acetonitrile display negative and positive Cotton effects at  $\lambda = 208$  and  $241$  nm (Figure 5c), while *rac*-4 does not show dichroic signal, demonstrating the chiral nature of *S*-4 and *R*-4, and racemic nature of *rac*-4. In addition, the dichroic signals of



*S-4* or *R-4* in acetonitrile did not change after the solution was stood at room temperature for over 1 month, indicating the separated *S-4* and *R-4* enantiomers are stable in acetonitrile. Thus *S-3/R-3* and *S-4/R-4* can be used as chiral starting materials for the constructions of homochiral metal organic frameworks (MOFs) and chiral catalysis.

In summary, we have demonstrated that a racemic nickel(II) complex  $[\text{Ni}(\alpha\text{-rac-L})](\text{ClO}_4)_2$  can be separated efficiently to two enantiopures of  $\Delta\text{-1}$  and *a-2*, and  $\Lambda\text{-1}$  and *b-2*, by the reactions of  $[\text{Ni}(\alpha\text{-rac-L})]^{2+}$  with *l*- and *d*-phenylalanine ( $\text{Phe}^-$ ), respectively. In addition, hydrogen bond linking of  $[\text{Ni}(f\text{-SS-L})(l\text{-Phe})]^+$  and  $[\text{Ni}(f\text{-RR-L})(d\text{-Phe})]^+$  monomers generate 1D right- and left-handed helical chains respectively, while the hydrogen bond linking of  $[\text{Ni}(f\text{-RR-L})(l\text{-Phe})]^+$  and  $[\text{Ni}(f\text{-SS-L})(d\text{-Phe})]^+$  monomers generate 1D zigzag chains. Furthermore, spontaneous resolution occurred when  $[\text{Ni}(\alpha\text{-rac-L})](\text{ClO}_4)_2$  reacted with racemic

*dl*- $\text{Phe}^-$ , and the mixture of enantiomers can self-sort through intermolecular hydrogen bonding interactions to generate a conglomerate of *c-1*. The results have demonstrated again that hydrogen bonds play a key role in the process of spontaneous resolution.<sup>10d</sup> At present, we are using enantiomers of *S-3* and *R-3* as building blocks to construct chiral helical chains and higher dimensional frameworks, as well as chiral catalysts for some organic reactions.

**Acknowledgment.** This work was supported by NSFC (20625103) and 973 Program of China (2007CB815305).

**Supporting Information Available:** File in CIF format, Table S1, and Figures S1–S4. This material is available free of charge via the Internet at <http://pubs.acs.org>.

IC7021424